UNRESOLVED Hα ENHANCEMENTS AT HIGH GALACTIC LATITUDE IN THE WHAM SKY SURVEY MAPS

R. J. Reynolds, V. Chaudhary, G. J. Madsen, and L. M. Haffner
Department of Astronomy, University of Wisconsin, Madison, WI 53706

ABSTRACT

We have identified 85 regions of enhanced Hα emission at $|b| > 10°$ subtending approximately $1°$ or less on the Wisconsin Hα Mapper (WHAM) sky survey. These high-latitude "WHAM point sources" have Hα fluxes of 10^{-11}–10^{-9} ergs cm^{-2} s^{-1}, radial velocities within about 70 km s^{-1} of the LSR, and line widths that range from less than 20 to about 80 km s^{-1} (FWHM). Twenty-nine of these enhancements are not identified with either cataloged nebulae or hot stars and appear to have kinematic properties that differ from those observed for planetary nebulae. Another 14 enhancements are near hot evolved low-mass stars that had no previously reported detections of associated nebulosity. The remainder of the enhancements are cataloged planetary nebulae and small, high-latitude H II regions surrounding massive O and early B stars.

Key words: catalogs — H II regions — planetary nebulae: general — subdwarfs — white dwarfs

1. INTRODUCTION

The Wisconsin Hα Mapper (WHAM) has provided the first large-scale survey of the distribution and kinematics of ionized interstellar hydrogen, covering the sky north of declination $-30°$ with an angular resolution of about $1°$ and a velocity resolution of 12 km s^{-1} within approximately ±100 km s^{-1} of the LSR (Haffner et al. 2003). This survey shows interstellar Hα emission filling the sky, with loops, filaments, and other large emission enhancements superposed on a more diffuse background. However, in addition to these large-scale features, the survey also reveals numerous small Hα emission regions that have angular sizes comparable to or less than WHAM's $1°$ diameter beam. In narrow (≈20 km s^{-1}) velocity interval maps, these WHAM point sources (WPSs) stand out as intensity enhancements in a single beam (or two adjacent beams) within a region of fainter diffuse emission.

Below we briefly describe our procedure for identifying and characterizing these enhancements, and we list the resulting flux, radial velocity, and line width of the Hα emission, along with any previously cataloged nebulosity or hot star that may be associated with the region. The nature of most of these emission regions is unknown.

2. IDENTIFICATION OF "WHAM POINT SOURCES"

The enhancements were identified through a systematic search by eye through the entire data cube of the WHAM survey. This consisted of examining regions of the sky approximately 100–400 deg^2 in size within narrow (20–30 km s^{-1}) radial velocity intervals centered between -90 and $+90$ km s^{-1} (LSR). To minimize confusion with structure within bright, larger scale emission features near the Galactic midplane, we confined the search to Galactic latitudes $|b| > 10°$. We also avoided the radial velocity interval from -15 to $+15$ km s^{-1} in directions toward the Orion-Eridanus bubble, where relatively bright high-latitude Hα emission features make the identification of "point sources" unreliable. A less subjective identification program was also carried out, which calculated for each of the approximately 37,000 survey spectra the difference between the spectrum in a given direction and the average spectrum of that direction's nearest neighbors. Directions with an enhancement were then selected on the basis of whether the difference spectrum exhibited an emission feature that was significantly greater than the scatter in the intensities of the nearest neighbors within the velocity range of the feature. This second method yielded a factor of 10 more "point source identifications." However, a cursory examination revealed that the vast majority of these were false positives associated with small angular scale fluctuations within the diffuse Hα background. We concluded that confidence in the identification of a true enhancement above the background required an examination by eye of a relatively large ($\sim10° \times 10°$) region of the surrounding sky, not just the six nearest neighbors. This allowed us to select only those enhancements that stood out most clearly against the background and was thus the more conservative approach. The survey was examined by two of us (V. C. and R. J. R.) independently, and the good agreement between the two results suggests that the enhancement identifications are robust, with Hα surface brightnesses measured down to about 0.3R (1R = $10^6/4\pi$ photons cm^{-2} s^{-1} sr^{-1}), corresponding to an Hα flux of about 1×10^{-11} ergs cm^{-2} s^{-1} for sources subtending $1°$. Although this Hα flux limit is not particularly low for a planetary nebula search, the surface brightness limit, corresponding to an emission measure of about 1 cm^{-6} pc, is well below that of most planetary nebula searches. The sensitivity of WHAM is further enhanced over low spectral resolution imaging in cases in which the enhancement is Doppler shifted with respect to the often higher surface brightness emission associated with the ubiquitous warm ionized component of the interstellar medium (see below).

The Hα flux, radial velocity, and line width associated with each enhancement was measured by subtracting from the spectrum toward the enhancement the average spectrum toward the nearest neighbors and then fitting the resulting Hα emission line with a Gaussian profile. Examples are presented in Figures 1–4, which show for four relatively faint enhancements the velocity interval beam map of an area surrounding the enhancement, the spectra in the source direction and its nearest neighbors, and the difference spectrum with the best-fit Gaussian and residuals. The intensity enhancements in these examples range from 1.3R (Fig. 1) down to 0.5R (Figs. 2 and 3) and, depending upon the brightness of the diffuse Hα background, produce moderate
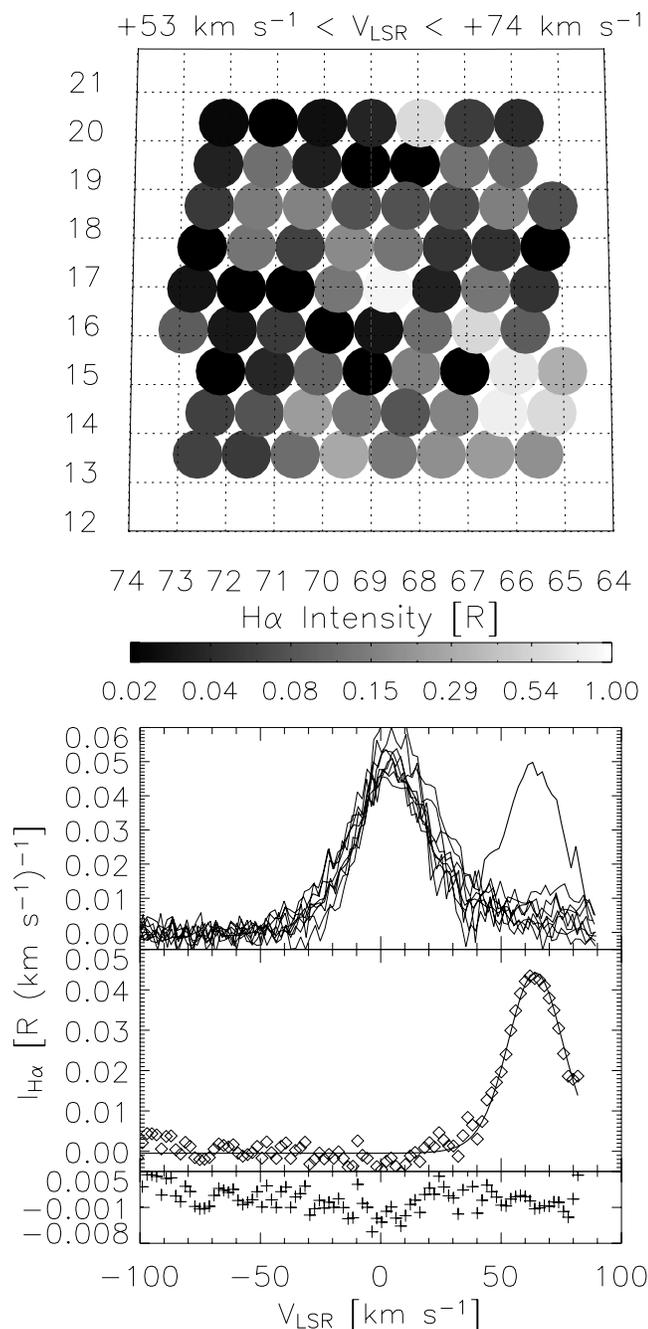
FIG. 1.—*Top*: Radial velocity interval map of a small portion of the WHAM Hα sky survey showing the intensity enhancement toward WPS 20 at $l = 68°.7$, $b = +17°.0$. The circles represent the WHAM beams, and the gray scale denotes the Hα intensity within each beam (in rayleighs). The coordinates are degrees of Galactic longitude (abscissa) and latitude (ordinate). *Bottom*: Hα spectra (*solid lines*) toward WPS 20 and its nearest neighbors, and the difference spectrum (*diamonds*) with its single-Gaussian best fit and residuals (*crosses*); see § 2 in text. The Hα line centered near 0 km s^{-1} in all of the spectra is emission associated with the widespread warm ionized component of the interstellar medium (e.g., Haffner et al. 2003).

(Fig. 2) to small (Fig. 4) increases in the total Hα intensity on the sky. The high spectral resolution of the WHAM survey has made possible the detection of sources (e.g., Fig. 4) that would be masked by the Hα background and its variation in maps of total Hα intensity. For these examples, there are no associations with previously reported nebulae (i.e., listed either in SIMBAD or in Cahn et al. 1992). In one of these examples (Fig. 2), the enhanced emission appears to be associated with a hot, evolved
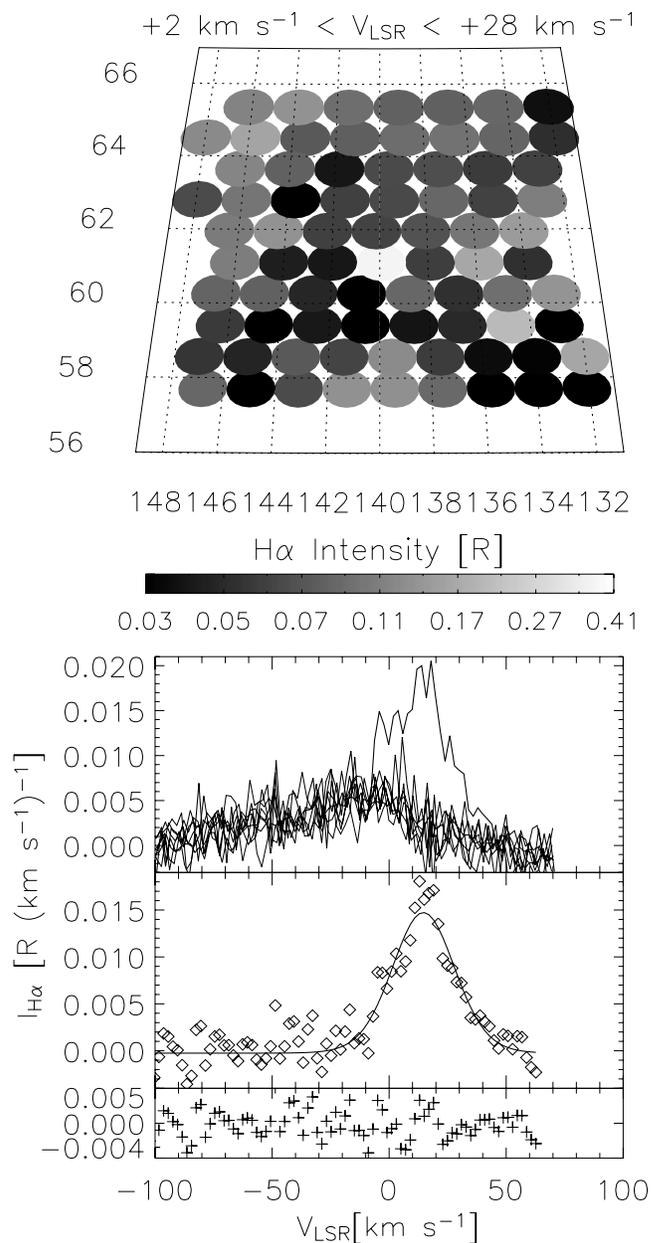
FIG. 2.—Same as Fig. 1, except for WPS 43.

low-mass star (DA white dwarf), whereas for the other three no cataloged hot star is associated with the ionized region (see § 3).

Seven of the enhancements occupy two adjacent pixels on the sky (e.g., Fig. 4), rather than being confined to a single WHAM beam. With one exception (WPS 6), we have assumed that these are situations in which the emission region is located near the edge of a beam, extending into the second beam. In these cases, we summed the two spectra, and the coordinates of the enhancement refer to the mean position of the two beams. For the 2 pixel source WPS 6 at $l = 33°.8$, $b = -22°.1$ and $l = 34°.1$, $b = -21°.2$, the results in Table 1 are listed separately for each beam because there is a significant velocity shift associated with the enhancement between the two directions (Fig. 5), suggesting two independent sources (see § 4).

3. RESULTS

Table 1 lists in order of increasing Galactic longitude the identified WPSs and the results of the Gaussian fits to the
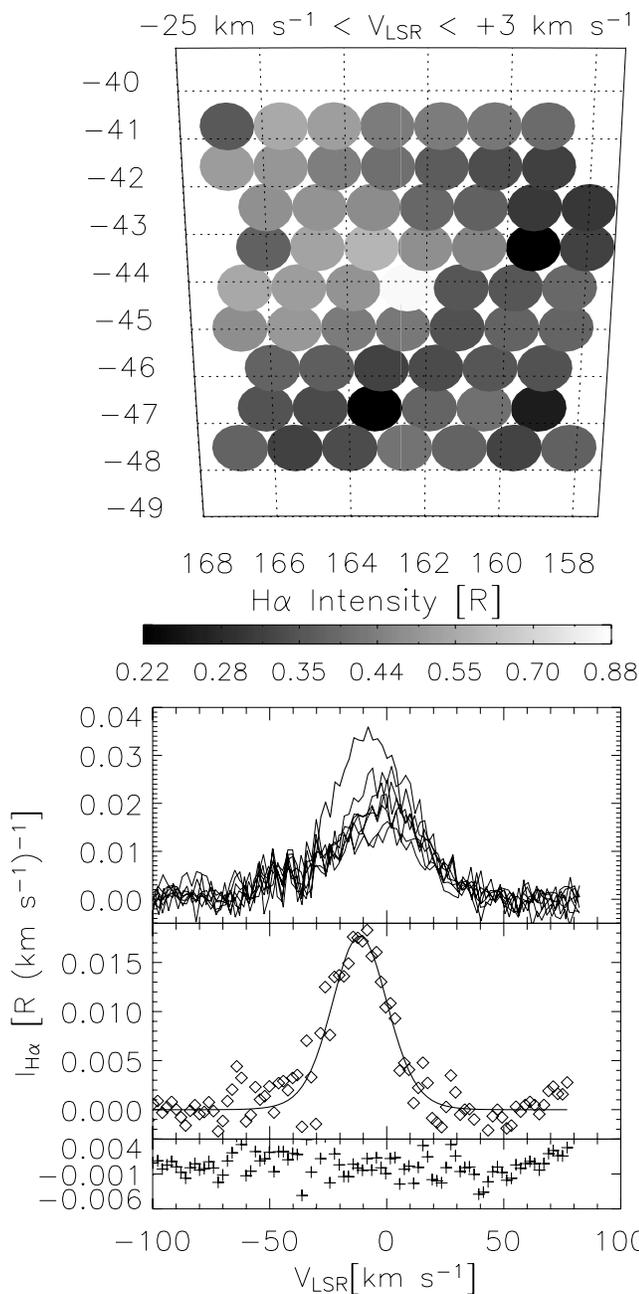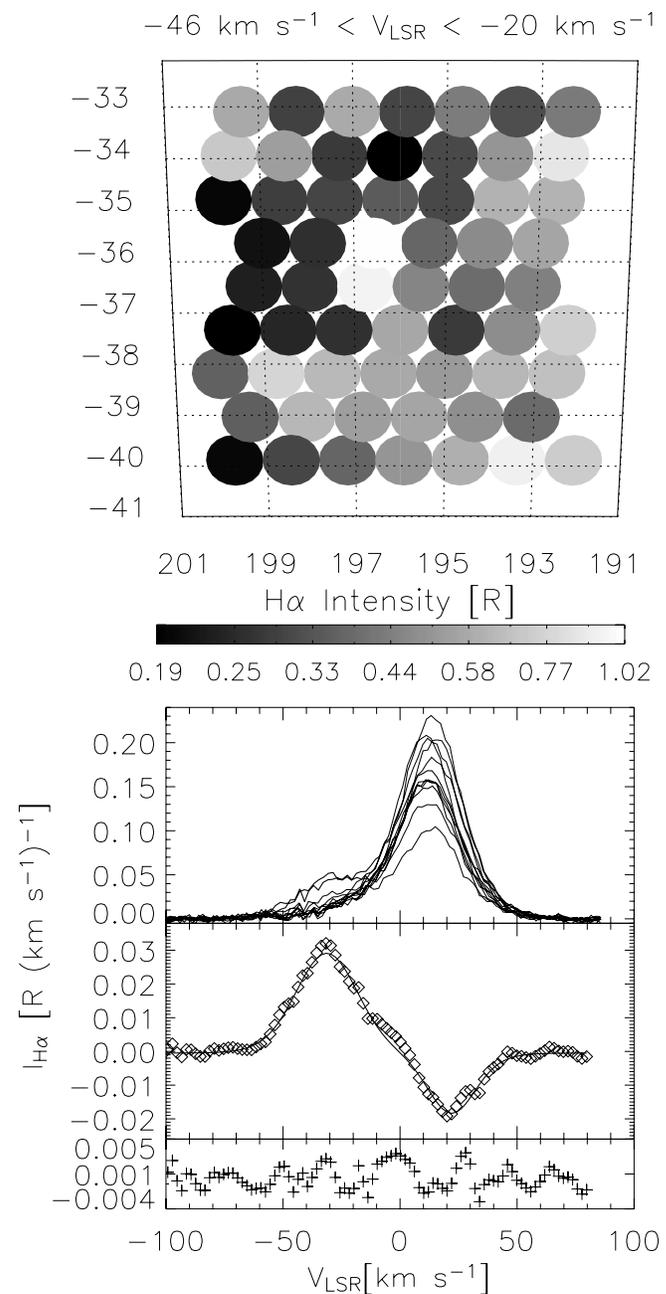
Fig. 3.—Same as Fig. 1, except for WPS 53.

Fig. 4.—Same as Fig. 1, except for WPS 63. Note that this is a 2 pixel enhancement. The parameters for this source listed in Table 1 refer to the positive-area Gaussian centered at about −30 km s⁻¹ in the difference spectrum.

difference spectra. Following the WPS number are the Galactic coordinates of the center of the WHAM survey beam (for single-pixel sources), plus the Hα flux, radial velocity, and line width (FWHM) for each of the enhancements. The enhancements WPS 6-1 and WPS 6-2, although in adjacent pixels, are treated as two separate H II regions (see § 4), whereas WPS 65 is a planetary nebula exhibiting two resolved Hα velocity components (Recillas-Cruz & Pişmiş 1981). The Hα flux is based on a calibration using those enhancements identified as planetary nebulae (see Table 2) and for which Hβ fluxes and reddening measurements have been published (Cahn et al. 1992). The errors in the fitted parameters are dominated by the uncertainty in the baseline of the difference spectrum and/or by the scatter in the data points of the spectrum (e.g., see Figs. 1–4). Errors due to baseline uncertainty were estimated by fitting each difference spectrum multiple times with different fixed

baselines. Errors due to scatter in the spectral data points were determined by the standard deviation calculation carried out by the least-squares Gaussian fitting program. The listed errors for each parameter represent the largest uncertainties determined by these methods.

Table 2 lists for each enhancement the celestial coordinates (J2000.0) of the center of the beam (or the mean position for 2 pixel sources), the name of any cataloged nebulae near that direction, the name of a candidate ionizing star (if there is no cataloged nebula), the spectral type of the star, and the offset of the nebula or star from the center of the beam. The resources for the ionizing star and nebula searches were SIMBAD and the planetary nebula catalog by Cahn et al. (1992). When no cataloged nebula was listed within 40′ of the beam center, a

RESULTS FOR HIGH-LATITUDE WHAM POINT SOURCES

WPS	l (deg)	b (deg)	$F_{H\alpha}$ (10^{-11} ergs cm^{-2} s^{-1})	V_{LSR} (km s^{-1})	FWHM (km s^{-1})
1............	23.14	−17.83	13.8 ± 1.7	+38 ± 1	39 ± 3
2............	23.76	−14.43	8.8 ± 0.8	+47 ± 1	18 ± 2
3............	25.87	+40.74	7.9 ± 0.8	+41 ± 1	29 ± 3
4............	26.20	+46.68	2.9 ± 1.3	−4 ± 6	56 ± 15
5............	26.23	−17.83	8.8 ± 1.7	+14 ± 2	43 ± 4
6-1[a].......	33.84	−22.07	5.0 ± 0.8	−10 ± 2	24 ± 4
6-2[a].......	34.13	−21.22	4.2 ± 1.3	+11 ± 2	25 ± 5
7............	35.05	+11.88	56.8 ± 1.3	+11 ± 1	35 ± 12
8............	36.35	−56.86	111.2 ± 2.5	−24 ± 1	40 ± 5
9............	37.49	−34.80	51.8 ± 4.2	−40 ± 2	45 ± 1
10...........	38.06	+11.88	5.4 ± 0.8	+39 ± 2	24 ± 4
11[b].......	39.84	−35.23	10.8 ± 1.7	+26 ± 3	25 ± 5
12[b].......	43.01	+37.77	40.1 ± 1.7	−20 ± 1	23 ± 2
13.........	44.77	−46.68	2.1 ± 0.4	−28 ± 4	34 ± 6
14.........	45.76	+24.61	2.9 ± 0.8	0 ± 2	22 ± 6
15.........	54.08	−11.88	10.9 ± 2.1	+48 ± 3	51 ± 4
16[b].......	55.00	−14.86	7.5 ± 1.7	+13 ± 2	21 ± 3
17.........	57.03	+43.28	8.4 ± 4.2	−69 ± 4	22 ± 12
18.........	58.40	−11.03	7.1 ± 2.1	−40 ± 7	39 ± 15
19.........	65.56	+22.07	2.9 ± 0.8	−37 ± 3	27 ± 10
20.........	68.65	+16.97	5.4 ± 0.8	+64 ± 1	21 ± 3
21.........	69.31	−18.67	6.3 ± 0.8	+52 ± 2	27 ± 4
22.........	69.42	−30.55	3.3 ± 0.8	+30 ± 4	36 ± 14
23.........	71.38	+18.67	9.2 ± 0.8	+17 ± 1	27 ± 4
24.........	72.75	−16.97	5.0 ± 0.8	+43 ± 5	23 ± 7
25.........	74.85	−36.49	4.6 ± 0.8	+10 ± 3	32 ± 5
26.........	83.73	+72.99	2.1 ± 0.8	−24 ± 5	37 ± 13
27.........	83.88	+12.73	47.2 ± 2.9	+13 ± 1	34 ± 1
28.........	91.99	+19.52	3.3 ± 0.8	+6 ± 3	27 ± 6
29.........	96.39	+29.70	78.6 ± 2.9	−55 ± 1	37 ± 1
30.........	106.52	−17.82	36.8 ± 1.3	−10 ± 1	49 ± 2
31.........	109.82	+21.22	7.5 ± 0.4	−22 ± 1	20 ± 2
32.........	110.16	−11.88	2.5 ± 0.8	+50 ± 4	31 ± 9
33.........	118.60	+39.04	2.5 ± 0.8	+15 ± 3	24 ± 8
34.........	118.75	−74.69	5.9 ± 2.1	+34 ± 10	73 ± 20
35.........	120.00	+18.67	7.1 ± 0.8	+4 ± 1	25 ± 1
36.........	123.41	+34.80	5.4 ± 0.8	−35 ± 2	34 ± 4
37.........	126.19	−46.68	1.7 ± 0.4	+6 ± 1	20 ± 3
38.........	130.75	−52.62	2.1 ± 0.8	−14 ± 3	21 ± 8
39.........	133.11	+12.73	4.6 ± 0.8	−33 ± 2	27 ± 5
40.........	133.22	−40.74	1.3 ± 0.4	−36 ± 4	22 ± 13
41.........	137.39	−24.61	5.4 ± 1.3	−63 ± 2	26 ± 3
42.........	139.24	+45.83	2.1 ± 0.8	−57 ± 7	47 ± 14
43.........	139.94	+61.11	2.1 ± 0.8	+15 ± 4	26 ± 11
44.........	142.11	−28.86	5.4 ± 1.3	−26 ± 4	58 ± 8
45.........	142.23	+15.28	1.3 ± 0.4	−79 ± 2	13 ± 4
46[b].......	143.86	+38.62	5.0 ± 0.8	−52 ± 2	31 ± 5
47.........	146.70	−23.76	2.9 ± 0.8	+30 ± 4	39 ± 7
48.........	149.29	+56.86	5.9 ± 1.7	+15 ± 5	79 ± 11
49.........	159.02	+17.82	5.9 ± 0.8	+7 ± 2	37 ± 5
50.........	159.02	+37.34	2.1 ± 0.8	−9 ± 5	28 ± 13
51.........	160.62	−23.76	11.3 ± 3.3	+9 ± 1	23 ± 2
52.........	161.20	−26.31	7.5 ± 1.3	+8 ± 1	22 ± 3
53.........	162.48	−44.13	2.1 ± 0.4	−11 ± 3	28 ± 7
54.........	162.55	+47.53	1.7 ± 0.8	−19 ± 5	38 ± 14
55.........	163.94	−16.97	13.8 ± 1.3	−6 ± 1	17 ± 1
56.........	164.68	+31.40	2.1 ± 8.4	−60 ± 5	44 ± 15
57.........	165.59	−15.28	4.2 ± 0.8	+42 ± 4	42 ± 10
58.........	166.28	+10.18	10.0 ± 0.8	−39 ± 1	31 ± 2
59.........	174.73	+15.28	10.0 ± 1.3	−33 ± 1	27 ± 3
60.........	181.26	+11.88	7.1 ± 1.3	−2 ± 1	24 ± 3
61.........	191.42	+40.74	1.7 ± 0.4	+5 ± 7	32 ± 19
62.........	193.44	−24.61	1.5 ± 2.9	−11 ± 1	14 ± 2
63[b].......	196.66	−36.07	9.2 ± 1.7	−33 ± 1	26 ± 2

WPS	l (deg)	b (deg)	$F_{H\alpha}$ (10^{-11} ergs cm^{-2} s^{-1})	V_{LSR} (km s^{-1})	FWHM (km s^{-1})
64..........	199.45	−22.92	4.2 ± 0.4	−63 ± 2	23 ± 4
65[c].........	204.90	+14.43	7.5 ± 0.8	+2 ± 3	22 ± 10
65[c].........	204.90	+14.43	6.3 ± 1.3	+39 ± 2	28 ± 8
66..........	211.31	+11.88	6.7 ± 0.7	+3 ± 1	20 ± 2
67..........	215.00	−24.61	100.7 ± 2.1	+44 ± 1	28 ± 2
68..........	216.18	−67.89	2.1 ± 0.8	−12 ± 5	34 ± 13
69..........	217.07	+28.86	11.7 ± 2.5	−3 ± 1	20 ± 2
70..........	218.64	+31.40	4.6 ± 1.3	+22 ± 3	54 ± 7
71..........	220.09	−54.31	11.3 ± 1.3	+49 ± 3	73 ± 5
72..........	223.71	−20.37	29.3 ± 1.7	−7 ± 1	17 ± 1
73..........	235.12	+47.53	1.7 ± 0.4	+16 ± 5	35 ± 12
74..........	235.17	+29.70	5.4 ± 0.8	+6 ± 2	25 ± 5
75..........	243.09	+36.49	2.5 ± 0.4	0 ± 3	24 ± 7
76..........	260.73	+32.25	48.1 ± 2.5	+1 ± 1	43 ± 1
77..........	264.29	+50.92	1.7 ± 0.4	−3 ± 5	26 ± 10
78..........	293.97	+43.28	7.5 ± 1.3	+12 ± 7	67 ± 15
79..........	303.20	+39.89	15.1 ± 0.4	−12 ± 1	28 ± 2
80..........	312.12	+67.05	2.5 ± 0.8	−23 ± 2	12 ± 7
81..........	315.00	+36.49	2.5 ± 0.8	+39 ± 5	40 ± 14
82[b]........	337.44	+47.53	6.7 ± 1.7	−17 ± 2	26 ± 5
83..........	347.06	+20.37	219 ± 29	+1 ± 1	21 ± 1
84..........	351.45	+16.97	493 ± 50	0 ± 1	20 ± 1

[a] Two pixel point source for which the radial velocity is different in each beam; see text.
[b] Two pixel point source.
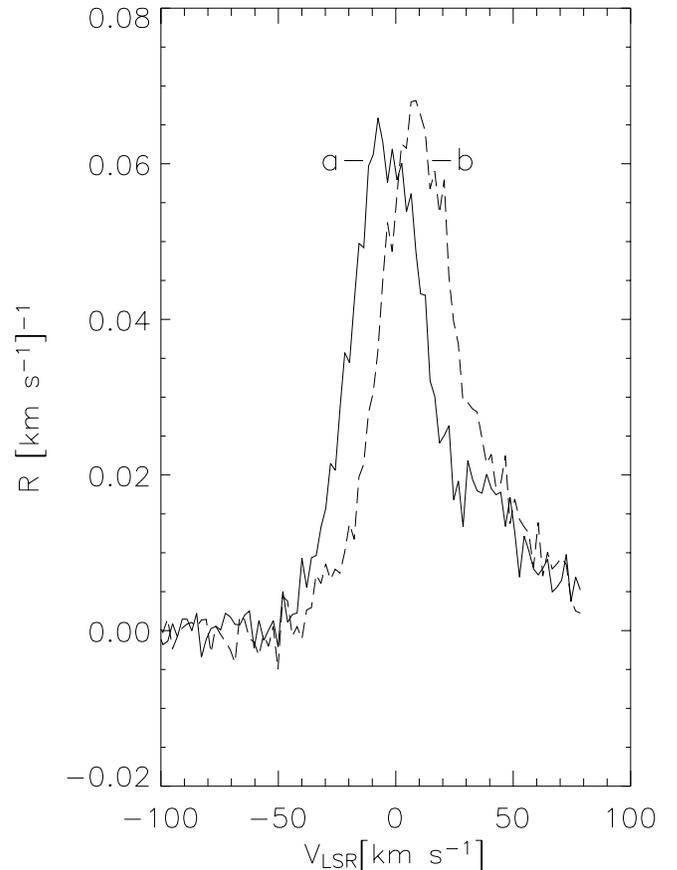[c] One pixel point source with two emission peaks.

FIG. 5.—Hα difference spectra toward WPS 6-1 and WPS 6-2. Line a: $l = 33°.8$, $b = −22°.1$; line b: $l = 34°.1$, $b = −21°.2$.

930

TABLE 2
WHAM POINT SOURCE IDENTIFICATIONS

WPS	R.A. (J2000.0)	Decl. (J2000.0)	Nebula	Star	Spectral Type	Beam Offset (arcmin)
1	19 39.3	−16 29	...	LSE 22	O+	56
2	19 27.4	−14 32	...	V4372 Sgr	B2 IV	38
3	16 12.8	+12 24	IC 4593	...	...	25
4	15 51.0	+15 05	...	PG 1548+149	DA	18
5	19 54.9	−13 48	NGC 6818	...	...	22
6	20 11.0	−08 48	...	HD 191639	B1 V	4
7	18 12.7	+07 15	NGC 6572	...	...	25
8	22 28.7	−20 40	NGC 7293	...	...	17
9	21 04.6	−11 40	NGC 7009	...	...	19
10	18 18.0	+09 53	PHL 932	...	...	16
11	21 09.6	−10 07	...	...	...	...
12	16 44.4	+23 44	NGC 6210	...	...	5
13	21 58.1	−11 55	...	...	...	...
14	17 41.7	+21 41	G045.6+24.3 (K1-14)	...	...	19
15	20 14.1	+12 44	NGC 6891	...	...	16
16	20 26.4	+11 54	...	...	...	...
17	16 29.3	+35 15	...	...	...	...
18	20 11.8	+13 27	IC 4997	...	...	5
19	18 20.3	+38 02	...	FBS 1815+381	DA	35
20	18 49.9	+39 03	...	...	...	...
21	21 12.9	+20 44	...	...	...	...
22	21 50.4	+12 57	LBN 069.67-30.36	...	...	16
23	18 46.4	+42 05	...	...	...	...
24	21 16.5	+24 20	PK 072-17 (A74)	...	...	7
25	22 20.7	+11 56	...	31 Peg	B2 IV−Ve	21
26	13 47.0	+39 38	...	...	...	...
27	19 46.1	+50 46	NGC 6826	...	...	19
28	19 24.9	+60 40	...	...	...	...
29	18 01.1	+66 34	NGC 6543	...	...	15
30	23 26.1	+42 19	NGC 7662	...	...	13
31	20 25.3	+76 40	...	KUV 20417+7604	sd:O	60
32	23 34.3	+49 04	PP105 (K1-20)	...	...	51
33	13 54.6	+77 33	...	...	...	...
34	00 46.9	−11 51	NGC 246	...	...	2
35	23 38.2	+81 07	LBN 120.29+18.39	...	...	26
36	12 39.7	+82 19	IC 3568	...	...	20
37	01 00.7	+16 08	PHL 932	...	...	26
38	01 10.7	+09 58	...	PG 0108+101	DO	25
39	03 13.4	+72 44	...	...	...	...
40	01 24.9	+21 28	...	PG 0122+214	sd?	12
41	01 57.0	+36 25	...	...	...	...
42	10 49.9	+67 16	...	...	...	...
43	11 55.6	+54 08	...	EGGR 435	DA	37
44	02 09.9	+31 04	...	...	...	...
45	04 53.3	+68 30	IRAS 04488+6903	...	...	28
46	09 25.8	+69 05	...	PG 0931+691	sd:O	57
47	02 37.3	+34 11	...	KUV 02335+3343	sdB	18[a]
48	11 11.7	+54 52	NGC 3587	...	...	29
49	06 19.6	+55 31	G158.9+17.8 (PW1)	...	...	6
50	08 42.6	+58 02	G158.8+37.1 (A28)	...	...	14
51	03 27.8	+27 27	...	...	...	...
52	03 22.7	+25 06	...	...	...	...
53	02 42.1	+10 05	...	...	...	...
54	09 48.4	+53 04	...	...	...	...
55	03 58.7	+30 37	...	X Per	O9.5pe	50
56	07 59.3	+53 33	G164.8+31.1	...	...	15
57	03 59.6	+32 44	NGC 1514	...	...	4
58	05 55.2	+45 51	IC 2149	...	...	19
59	06 40.1	+40 37	...	WD 0632+40	DA	45
60	06 37.4	+33 27	...	...	...	...
61	09 02.6	+33 01	...	CBS 90	DA	35
62	04 48.6	+04 36	HS 0444+453	...	...	35
63	04 16.9	−03 34	...	...	...	...
64	05 05.9	+00 47	...	...	...	...
65	07 29.3	+13 32	G205.1+14.2 (YM29)	...	...	18
66	07 31.0	+06 48	...	...	...	...
67	05 25.9	−12 39	IC 418	...	...	23

TABLE 2—*Continued*

WPS	R.A. (J2000.0)	Decl. (J2000.0)	Nebula	Star	Spectral Type	Beam Offset (arcmin)
68......................................	02 30.4	−26 12	...	...	...	...
69......................................	08 42.2	+09 26	...	...	...	...
70......................................	08 53.9	+09 19	PK 219+31 (A31)	...	...	25
71......................................	03 31.5	−25 47	NGC 1360	...	...	25
72......................................	05 55.6	−18 21	...	...	...	...
73......................................	10 15.5	+06 17	...	WD 1010+064	DA	31
74......................................	09 16.7	−03 49	...	PG 0914+037	sd:O	10
75......................................	09 54.6	−05 04	...	...	...	...
76......................................	10 24.6	−18 19	NGC 3242	...	...	20
77......................................	11 18.4	−04 50	...	...	...	...
78......................................	12 23.5	−19 23	NGC 4361	...	...	22
79......................................	12 52.3	−22 59	G303.6+40.0 (A35)	...	...	18
80......................................	13 05.8	+04 26	...	...	...	...
81......................................	13 34.3	−25 22	...	EC 13331-2540	sd:B	40
82......................................	14 22.6	−09 08	...	G124-26	DA	17
83......................................	15 57.9	−26 07	...	π Sco	B1 V	13
84......................................	16 21.7	−25 31	...	σ Sco	B1 III	8

Note.—Units of right ascension are hours and minutes, and units of declination are degrees and arcminutes.
[a] WD 0230+343 (DA) is within $52'$ of beam center.

search for an ionizing star was carried out on SIMBAD to a radius of $60'$.

4. DISCUSSION

Of the 85 Hα enhancements identified, more than half (44) are not associated with any previously cataloged nebula, and of these, 15 are associated with hot, evolved low-mass stars, including one DO and seven DA white dwarfs, three sdO stars, and two sdB stars (Table 2). This is a potential source of new information about the natures of these evolved stars and their evolution (Tweedy & Kwitter 1994). For example, because of WHAM's large beam, some of these enhancements could be associated with large planetary nebulae in very late stages of their evolution having surface brightnesses that are too faint to have been detected on earlier searches. The identification of the nebulosity with the star is most certain for those stars within the WHAM beam (i.e., angular offsets less than $30'$). However, because large, highly evolved planetary nebulae can be offset significantly from their ionizing stars (Tweedy & Napiwotzki 1994; Borkowski et al. 1990; Reynolds 1985), we have considered stars located up to $1°$ from the directions listed in the tables. We confirm the earlier detection of ionized gas associated with the DO white dwarf PG 0108+101 (Reynolds 1987) and provide improved kinematic information about that H II region.

Twenty-nine emission regions could not be associated with either a cataloged nebula or hot star. This could be the result of incompleteness in the SIMBAD listings, or it could indicate another kind of nebulosity. These enhancements have a mean line width near 27 km s^{-1}, significantly smaller than that (38 km s^{-1}) of the cataloged planetary nebulae. This is illustrated in Figure 6, which compares histograms of line widths for three categories of WHAM point sources: enhancements not associated with any cataloged nebula or evolved hot star, enhancements near a hot low-mass star, and enhancements associated with cataloged planetary nebulae. (The six regions associated with massive O and B stars are excluded from these histograms.) We found no associations with supernova remnants or Herbig-Haro objects, although WPS 11 and WPS 21 are within $37'$ and $48'$ of the two high Galactic latitude molecular clouds
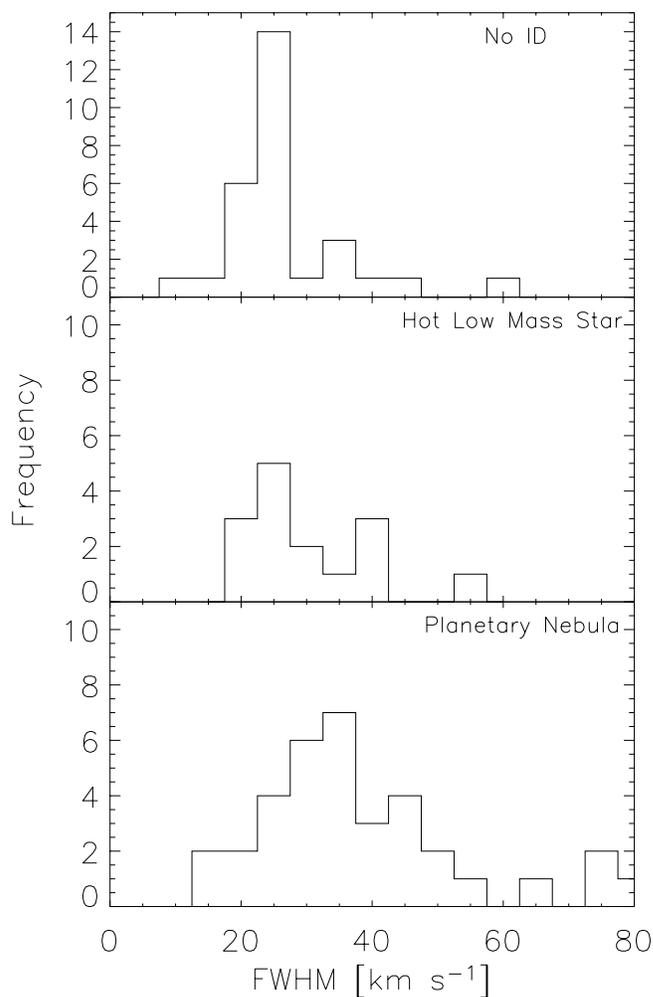

Fig. 6.—Histograms of the number of enhancements vs. FWHM of the Hα emission line. *Top*: Enhancements not associated with any previously cataloged nebula or any identified ionizing source. *Middle*: Enhancements not associated with any previously cataloged nebula but with a hot evolved low-mass star located within $1°$ of the center of the WHAM beam. *Bottom*: Enhancements associated with cataloged planetary nebulae.
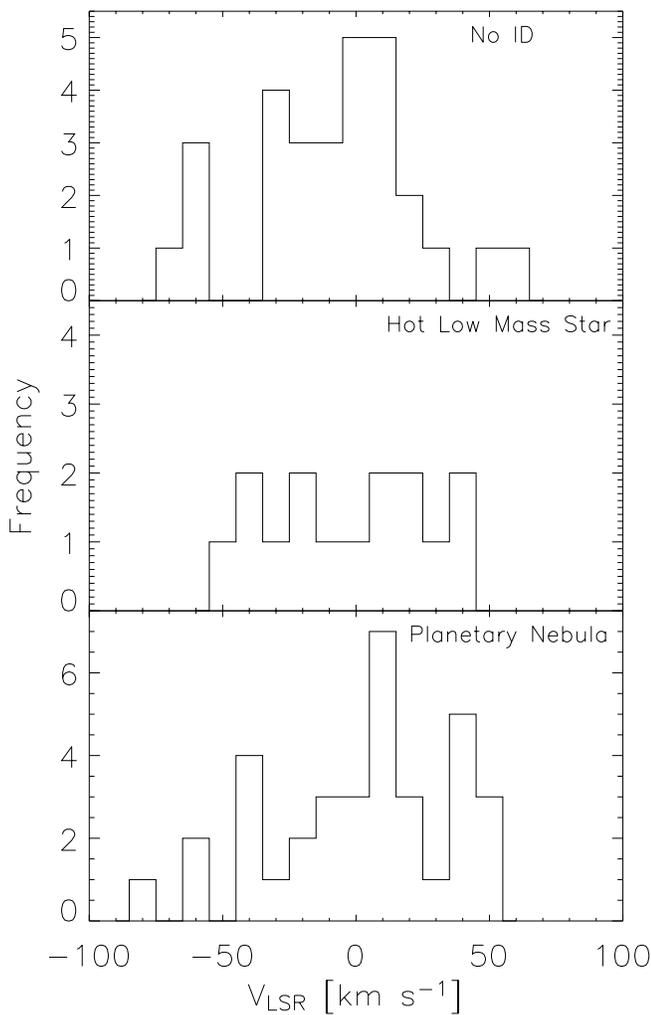
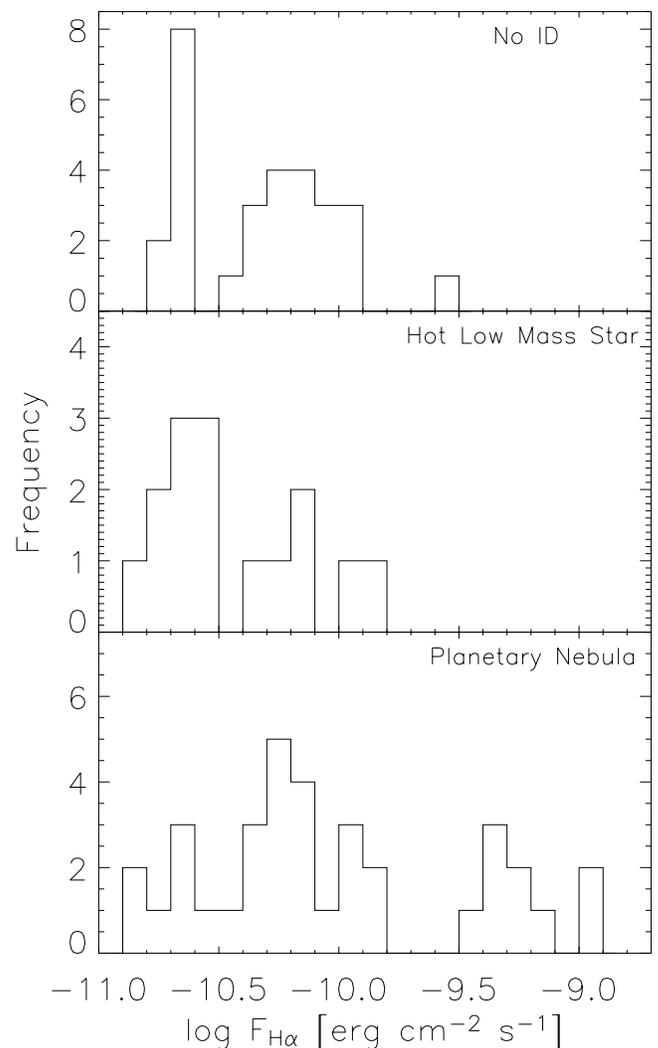FIG. 7.—Same as Fig. 6, except for histograms of the radial velocity of the Hα emission.

FIG. 8.—Same as Fig. 6, except for histograms of the flux of the Hα emission.

MBM 50 and MBM 46, respectively, which could harbor star formation activity. However, the narrow line widths appear to rule out such shock-excited sources, as well as any association with emission-line stars, which exhibit line widths in excess of 60–100 km s^{-1} (e.g., Hartigan et al. 1987; Hamann & Persson 1992a, 1992b). It is tempting to speculate that these emission regions are associated with the most evolved planetary nebulae, those whose expansion has been halted by interactions with the ambient interstellar medium (Tweedy & Napiwotzki 1994; Reynolds 1985) or those whose gas has thinned to such an extent that it is the ambient interstellar medium itself that has become the primary H II region (Borkowski et al. 1990). Follow-up, high angular resolution imaging of these regions could help to discriminate between the possibilities (Soker et al. 1991). Figures 7 and 8 show corresponding histograms for radial velocity and Hα flux. No clear differences between the three categories of enhancements are apparent in these distributions. In Figures 6, 7, and 8, the V_{LSR} and FWHM used for WPS 65 are the flux-weighted average radial velocity (i.e., +19 km s^{-1}) and the separation (i.e., 37 km s^{-1}) of the two velocity components, respectively.

Six of the enhancements appear to be small H II regions associated with massive late O- and early B-type stars. The region near the B1 V star HD 191639 (WPS 6) was detected in 2 pixels and exhibits a significant (21 km s^{-1}) radial velocity difference between the two directions (Fig. 5). This suggests either peculiar, small-scale kinematic variations within the region or the existence of two independent H II regions closely spaced on the sky. In this latter case, because the B star has a radial velocity of -7 ± 5 km s^{-1} (Wilson 1953), the emission region produced by the B star would be more likely associated with the enhancement (WPS 6-1) at -10 ± 2 km s^{-1} toward $l = 33°.8$, $b = -22°.1$, whereas the emission (WPS 6-2) at +11 km s^{-1} toward $l = 34°.1$, $b = -21°.2$ would have no identified source of ionization (for Figs. 6, 7, and 8, we have assumed this latter case). Enhancements WPS 23, 60, 68, and 72 have late B stars (B6 V, B9, B9, and B8/B9 II, respectively) located $34'-43'$ away. Because the Lyman continuum fluxes from such late-type B stars are predicted to be orders of magnitude weaker than the fluxes of the early B stars discussed above, we have concluded that these associations are coincidences.

5. SUMMARY AND CONCLUSIONS

From the WHAM sky survey we have identified and measured the fluxes, radial velocities, and line widths for 85 regions of Hα enhancement at Galactic latitudes $|b| > 10°$ that appear to subtend approximately 1° or less on the sky. Most of these ionized regions have not been previously reported as emission nebulae, and their nature is unknown. A next step is to carry out

additional observations to determine the morphology of these emission regions and their sources of ionization. This will include spectra of [O III] $\lambda 5007$, [N II] $\lambda 6584$, and [S II] $\lambda 6716$ to explore the ionization and excitation state of the gas, as well as observations using WHAM's "imaging mode" to obtain deep, very narrowband (30 km s^{-1}) images of these enhancements at an angular resolution at about $3'$ within a $1°$ field of view (Reynolds et al. 1998).

REFERENCES

Borkowski, K. J., Sarazin, C. L., & Soker, N. 1990, ApJ, 360, 173
Cahn, J. H., Kaler, J. B., & Stanghellini, L. 1992, A&AS, 94, 399
Haffner, L. M., Reynolds, R. J., Tufte, S. L., Madsen, G. J., Jaehnig, K. P., & Percival, J. W. 2003, ApJS, 149, 405
Hamann, F., & Persson, S. E. 1992a, ApJS, 82, 247
———. 1992b, ApJS, 82, 285
Hartigan, P., Raymond, J., & Hartmann, L. 1987, ApJ, 316, 323
Recillas-Cruz, E., & Pişmiş, P. 1981, A&A, 97, 398
Reynolds, R. J. 1985, ApJ, 288, 622

Reynolds, R. J. 1987, ApJ, 315, 234
Reynolds, R. J., Tufte, S. L., Haffner, L. M., Jaehnig, K., & Percival, J. W. 1998, Publ. Astron. Soc. Australia, 15, 14
Soker, N., Borkowski, K. J., & Sarazin, C. L. 1991, AJ, 102, 1381
Tweedy, R. E., & Kwitter, K. B. 1994, ApJ, 433, L93
Tweedy, R. E., & Napiwotzki, R. 1994, AJ, 108, 188
Wilson, R. E. 1953, General Catalogue of Stellar Radial Velocities (Washington: Carnegie Inst.)